Evolutionary Computing and Optimal Design of MEMS

P. Di Barba, *Member, IEEE,* S. Wiak, *Member, IEEE*

Abstract— **Fostered by the development of new technologies, micro-electro-mechanical systems (MEMS) are massively present on board of vehicles, within information equipment as well as in medical and healthcare equipment. A smart approach to the design of MEMS devices is in terms of the simultaneous optimization of multiple objective functions subject to a set of constraints. This leads to the family of solutions minimizing the degree of conflict among the objectives (Pareto front). Accordingly, in the paper a procedure of optimal shape design of MEMS based on evolutionary computing is proposed and validated on three case studies.**

Index Terms— **Field analysis and synthesis, finite-element method, multi-objective optimal shape design, MEMS, comb-drive electrostatic microactuator, magnetic micromirror, pancake inductor.**

I. Introduction

OPTIMIZATION plays a key role in the design of any device or system, and MEMS are no exception. The issue is to find a design space for a device which will satisfy the performance specifications. Often, they include several design criteria which cannot all be met at the same time. In this case, a designer is supposed to decide how the criteria should be ranked. This leads to the concept of multi-objective optimization, *i.e.* a search which attempts to satisfy several goals simultaneously: the theoretical background is based on the Pareto optimality theory [1].

While the basic concept of optimization – *i.e.* find the minimum or maximum value of an objective function dependent on a set of variables – is fairly obvious, implementing this process under the frame of the design procedure of a MEMS device is not obvious. From the very beginning, the goal of the process should be clearly defined: for instance, a design process of a device may well have as its goal an improvement in an existing prototype, rather than obtaining the best possible device.

Computational cost is another critical issue: in fact, a feasible combination of design variables requires at least one field analysis to determine its performance; this task can be computationally expensive, because electromagnetic analysis is based on two- or three-dimensional finite-element models. Moreover, field analysis might imply the numerical solution to costly problems, like *e.g.* multiphysics problems which in turn might be non-linear or time-dependent.

As far as algorithms are concerned, within a design space which is approximated to be locally quadratic, the gradient information can be used to drive the search from a guess solution towards a local optimum. This is known as a deterministic optimization process, and the optimal direction to move in can be determined by a minimization process such as the sequential quadratic programming [3]. However, the gradient may not be directly available from a numerical solution; therefore, such a process is difficult to implement. In addition, it converges to the local minimum nearest to the starting point. As an alternative, the design space could be sampled according to a stochastic law around the current point: if a better point nearby is found, then this is used as the updated current solution. There are several gradient-free approaches which have been developed, and the most popular are those based on evolutionary algorithms which attempt to mimick biological adaptation [2]; in fact, they have proven to be able to approximate the region where the global optimum is located.

The impressive advance of technology at both the micrometer and nanometer scales requires the development of powerful and flexible modelling tools to help the designer of devices and systems [7],[10],[16]. For instance, in [14] a topology optimization method to design a piezoelectrically-driven microgripper is proposed: four design criteria are considered, and the two-dimensional Pareto fronts trading off various pairs of criteria are identified by means of a genetic algorithm. A different approach to a similar subject was investigated in [20]. In turn, in [19] the design optimization of an electromagnetic valve actuator is proposed, and a suitable combination of three design criteria is exploited. In [15] the magnetic field in a permanent-magnet spherical motor at no-load is recovered, after inverting the magnetic induction measured along an accessible surface; the final aim is to compute the on-load torque by means of the Lorentz's law.

In a sense, it appears that the impact of modern numerical methods on MEMS design has been rather limited so far; a contribution to bridge this gap is here proposed. The paper is organized as follows; after a review of field-based multiobjective optimization theory, a procedure of evolutionary computing is proposed and used to solve three

Manuscript submitted xxx.
P. Di Barba is with Department of Industrial and Information Engineering, University of Pavia, via Ferrata 1, 27100 Pavia, Italy (e-mail: paolo.dibarba@unipv.it).
S. Wiak is with Institute of Mechatronics and Information Systems, Łódź University of Technology, ul. Stefanowskiego 18/22, 90-924 Łódź, Poland (e-mail: slawomir.wiak@p.lodz.pl).

case studies: the improvement of an electrostatic comb-drive microactuator, the magnetic actuation of a micromirror, and the induction heating of a graphite disk for Si wafer epitaxial growth, respectively.

II. Multiobjective formulation of a MEMS design problem

In engineering practice, a designer usually has to consider multiple objectives to fulfil at a time in the design of a device or a system, while the presence of a single objective is somewhat an exception or a simplification. There is a number of reasons for that:

- in general, industrial problems have multiple solutions which fulfil objectives and constraints, thus multiple optimal solutions arise;
- often, in industrial applications, some solutions can be preferred to others, so it is better to get a spread of feasible solutions from the design procedure rather than a single solution;
- when a set of optimal solutions is available, the selection is left to an external decision maker (usually, the designer) who can express his or her final preference.

In fact, design problems arising in MEMS design often exhibit multiple objective functions to be optimized simultaneously. Formally, considering n_v variables, a multiobjective optimization problem can be cast as follows:

$$\text{given } x_0 \in \Re^{n_v}, \text{ find } \inf_x F(x) \ , \ x \in \Re^{n_v} \tag{1}$$

fulfilling n_c inequality and n_e equality constraints

$$g_i(x) \le 0 \ , \ i = 1, n_c \tag{2}$$

$$h_j(x) = 0 \ , \ j = 1, n_e \tag{3}$$

and also $2n_v$ side bounds

$$\ell_k \le x_k \le u_k \ , \ k = 1, n_v \tag{4}$$

Equations (1)-(4) are subject to the solution of the relevant field analysis problem [4]; in general, those referred to are boundary-value problems governed by Maxwell's equations of electromagnetic field, as well as Fourier's equation of heat transfer and Lamé's equation of elasticity [13]. When two, or more, physical domains coexist and interact in the same device, a coupled-field – or multiphysics – problem is originated.

In (1), $F(x) = \{f_1(x), ..., f_{n_f}(x)\} \subset \Re^{n_f}$ is the objective vector composed of $n_f \ge 2$ terms. Therefore, F defines a transformation from the design space $\Re^{n_v}$ to the corresponding objective space $\Re^{n_f}$. Often, the n_f objectives have different physical dimensions: they might refer to various characteristics or performances of the device (*e.g.* cost of materials, device volume, field homogeneity, power loss and so forth), to be optimized simultaneously. Therefore, the designer is forced to look for best compromises among all the objectives. In order problem (1)-(4) to be non-trivial, the pair ($f_i(x)$, $f_j(x)$) must represent conflicting objectives for $i \ne j$; in other words, a solution $\tilde{x}$ minimizing all the objectives simultaneously does not exist. A survey of the state-of-the-art of optimal design methods in electromagnetism can be found *e.g.* in [5]. The proposed method of multiobjective optimal design of MEMS, based on algorithms of evolutionary computing, aims at approximating the most general solution to problem (1)-(4) in terms of the Pareto front of non-dominated solutions, *i.e.* those for which the decrease of an objective function is not possible without the simultaneous increase of at least one of all the other objective functions. Basically, this means to have a family of optimal solutions to be compared; *a posteriori*, the designer can select a single solution according to extra criteria of decision making.

III. Field-based optimal shape design

In a shape design problem, design vector x represents the geometric variables of the device to be optimized. This feature in itself makes the dependence of the j-th objective f_j , $j = 1, n_f$, rather complex. In fact, both the direct problem, through field equations, and the optimization problem, through objective functions, depend on geometry x. As a consequence, since objective f_j is usually a field-based quantity, it depends on x explicitly and also implicitly, by means of the field solution s(x). In general, the following mapping applies:

$$\{x\} \to s(x) \to f_j(x, s(x)) \ , \ j = 1, n_f \tag{5}$$

Accordingly, the minimization problem correctly reads:

$$\text{find } \inf_x f_j(x, s(x)) \ , \ x \in \Omega \subseteq R^{n_v} \ , \ j = 1, n_f \tag{6}$$

In a problem of shape design, in fact, two aspects are always involved: the optimal synthesis of field s which takes place in the device, and the optimal design of device geometry x; formulation (6) points out that these two aspects are tightly interconnected. The situation is even more complicated, because inequality constraints might be prescribed for the field; in other words, a set

$$C = \{s(x) \mid g_k(x, s(x)) \le c_k \ , \ c_k \in \Re \ , \ k = 1, n_c\} \tag{7}$$

can be defined. In this case, the minimization problem reads like (6) subject to (7), *i.e.* $s(x) \in C$. The form of the j-th objective function f_j suggests a way to classify shape design problems; in fact, it might represent the discrepancy between computed and prescribed value, or the value of a local quantity (*e.g.* a field component in a part of the device) or, more generally, some characteristics of the device, like weight or volume or cost. The solution to (6) is quite troublesome: in fact, function f_j may be neither differentiable nor convex; from the numerical viewpoint, f_j could be non-smooth a function. Moreover, the function evaluation in (6) or the constraint evaluation in (7) is costly, because any function call requires at least a solution to the field equation, which might be a non-linear one. This is the main source of insidiousness for field-based optimization problems, which calls for a trade-off among accuracy, runtime, and storage.

From the numerical viewpoint, the solution of optimal design problems requires, as a rule, a module for calculating the field, associated with a module performing the minimization of an objective function. Usually, field analysis can be performed either by differential methods originating from Maxwell's equations: finite-difference method (FDM), finite-element method (FEM), or by integral methods amenable to Green's theorems: boundary element method (BEM). In turn, numerical minimization can be achieved by means of deterministic or evolutionary methods; the combination of any method for analysis and any method for minimization gives origin to families of iterative procedures for solving an optimal design problem. Nowadays, most of commercially available codes devoted to electromagnetic field analysis are based on the FEM: in fact, it offers a general-purpose and flexible tool of field simulation.

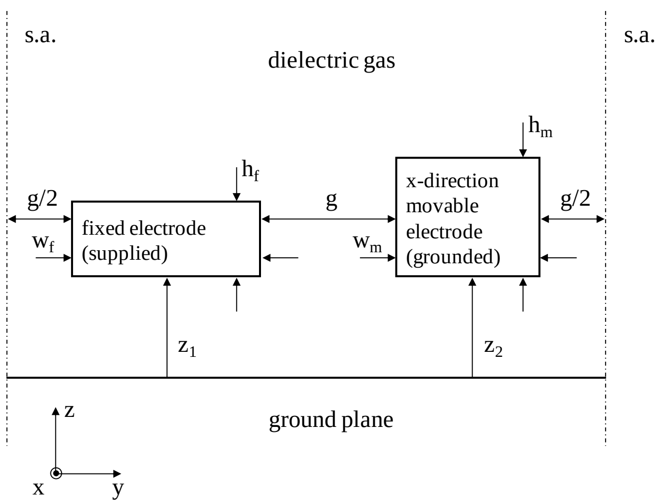

Fig. 1 Comb-drive cross-sectional view (fixed and movable electrode pair).

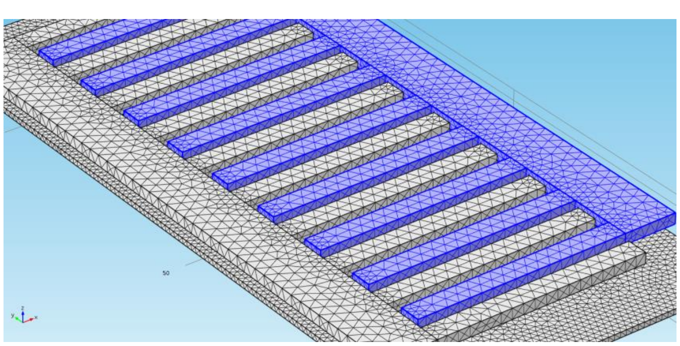

Fig. 2 Mesh detail of the comb drive model.

The proposed method of optimal design of MEMS has been validated by means of three case studies. Always, the field analysis problem relies on FEM, while the optimal design problem is solved by means of non-dominated sorting genetic algorithm (NSGA-II), a popular algorithm of evolutionary multiobjective optimization [6],[23]. Starting from an initial population of individuals distributed in the feasible design space, the Pareto criterion of non-dominated solution is applied to each individual in order to generate a suitable off-spring. The population is sorted according to the level of non-domination by applying a rank value depending on the front they belong to. Next, a crowding distance operator is used to maintain the diversity of the population. Finally, the individuals are selected based on their rank value and crowding distance.

IV. Case study: electrostatic comb-drive microactuator

A. Device model

A prototype model of comb drive device (Fig. 1), characterized by (w_m, w_f, h_m, h_f) = (4,4,2,2) [μm], where w and h are width and height of the movable (m) and the fixed (f) electrodes, respectively, is assumed as the first case study [8]. The device exhibits 10+9 electrodes and the corresponding distribution of electric potential u is shown in Fig. 3. The geometry of the device are amenable to the lumped-parameter model proposed in [9]. Moreover, the fixed and movable electrodes of the comb drive are 2 μm thick and 4 μm wide, respectively; the air-gap distance g between them is 2 μm wide, the same as their distance $z_1 = z_2$ from the grounded substrate.

B. Field analysis of the prototype

The equation governing the analysis problem of the modelled device is the Laplace's equation of the electric scalar potential u in the computational domain. Second-order Lagrangian shape functions were considered in the finite-element model: a typical mesh (Fig. 2) is composed of 170,000 elements with 240,000 unknowns [21], approximately. The device is considered electrically isolated: the boundary condition of the air subdomain is set to zero charge density; moreover, the fixed electrodes are at the same potential as the grounded substrate, while the movable electrodes are subject to voltage u_0 = 1 V. The device components are made of poly-cristalline Si exhibiting a relative permittivity ε_r = 4.5. In addition to the drive force in the direction of electrodes (shortly, x-directed drive force), the force due to electric field in the orthogonal direction (shortly, z-directed levitation force) takes place. The two force-displacement curves (drive and levitation, respectively) have been computed by means of the Maxwell's stress tensor method, taking the surface of the grounded electrodes as the integration surface. The elementary displacement was equal to 1 μm in the x direction (14 steps) and 0.3 μm in the z direction (7 steps): results are shown in Fig.s 4 and 5, respectively. The calculated force values are in agreement with reference values [10]; in particular, the approximated model $F_z = k(z\text{-}z_0)$ holds for the levitation term: k is named “electrostatic spring” constant, *i.e.* the z-directed force density per unit voltage [$NV^{-2}m^{-1}$], while z_0 is the equilibrium height of the movable electrode in the absence of a return spring force, *i.e.* the height towards which the electrodes spontaneously tend to move.

It can be remarked that the drive force abruptly decreases for small displacements between fixed and movable electrodes (Fig. 4), while for larger displacements it tends to be constant. Moreover, according to the levitation force *vs* angle curve, the equilibrium point z_0 is located at 1.2 μm with respect to the substrate (Fig. 5).

C. Field synthesis

A comb-drive actuator needs to be as coplanar as possible with respect to its sets of movable and fixed electrodes. To this end, various solutions have already been considered [11]. In the case study, a grounded substrate is laid under the set of electrodes as an attempt to cancel the vertical force. This way, however, the electric field distribution is no longer symmetric and the movable electrodes tend to levitate when the comb drive is energized. This vertical perturbation must be kept as low as possible while simultaneously the drive force should be increased.

Therefore, the ultimate goal of the optimal shape design problem is to find the family of geometries which maximize the x-directed drive force between movable and fixed electrodes, and simultaneously minimize the z-directed levitation force: a bi-objective optimization problem is so originated. To this end, the four-dimensional vector a = (w_m, w_f, h_m, h_f) of design variables has been defined; they are discrete-valued (step 0.1 μm) and can range from 2 to 8 μm.

Moreover, a two-dimensional vector F = (f_1, f_2) of objective functions has been defined, such that:

1. drive $f_1(a) = F_x(x,a)$ for z = 0 and $0 \le x \le 14$ μm, to be maximized with respect to vector a;
2. levitation $f_2(a) = F_z(z,a)$ for x = -13 μm and $0 \le z \le 1.8$ μm, to be minimized with respect to vector a.

In practice, the average value of the F_x *vs* x curve (Fig. 4) is maximized, and simultaneously the slope of the F_z *vs* z-displacement curve was minimized (Fig. 5).

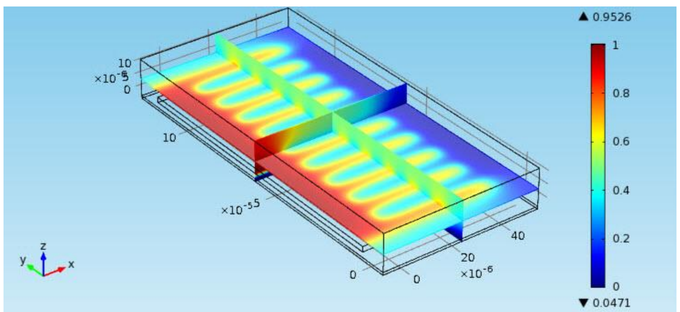

Fig. 3 Plot of the electric potential map.

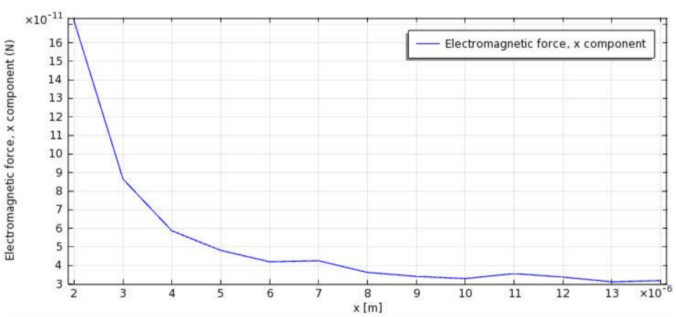

Fig. 4 Drive force $F_x(x)$ *vs* x-displacement.

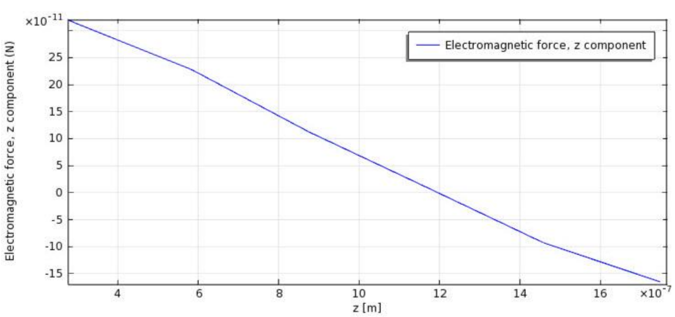

Fig. 5 Levitation force $F_z(z)$ *vs* z-displacement.

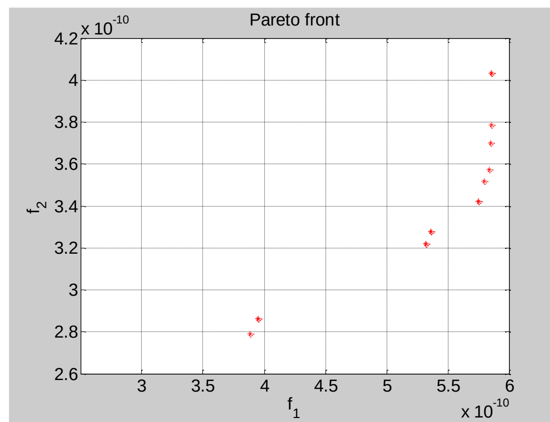

Fig. 6 Approximated Pareto front (f_1 - F_x force [N], f_2 - slope of F_z ***vs*** z displacement [N/μm]).

TABLE I
OPTIMAL SOLUTIONS TRADING OFF DRIVE AND LEVITATION

Width of movable electrodes w_m [μm]	Width of fixed electrodes w_f [μm]	Height of movable electrodes h_m [μm]	Height of fixed electrodes h_f [μm]	F_x drive force [N]·10^{-10}	Slope of F_z vs. z [N/μm]·10^{-10}
6	6	6.2	6.1	3.8848	2.7915
7.7	7.8	7.7	7.8	5.8568	4.0328
7.1	7.3	7.5	7.4	5.3189	3.2187
6.1	6.1	6.2	6.1	3.9496	2.862
7.6	7.7	7.8	7.9	5.8543	3.7876
7.7	7.7	7.8	7.8	5.8491	3.702
7.6	7.8	7.7	7.8	5.8385	3.5745
7.1	7.2	7.5	7.4	5.3614	3.2781
7.5	7.7	7.7	7.8	5.7529	3.4235
7.7	7.8	7.7	7.8	5.7975	3.5168

D. Optimal design results

The initial number of individuals processed was set to 15; the optimization procedure was stopped after 10 generations: this way, 10 non-dominated solutions approximating the Pareto front were identified (Fig. 6 and Table I).

V. CASE STUDY: MAGNETIC ACTUATION OF A MICROMIRROR

A micromagnetic device used as an optical switch [17],[18] is considered (Fig. 7) as the second case study: it consists of a NdFeB magnet, two conductors carrying like currents, and a ferromagnetic plate free to rotate around its axis. The residual induction of magnet is 1.2 T, while values of relative magnetic permeability equal to 10^3 and 1.05 are assumed for plate and magnet, respectively; moreover, the depth of the model is w = 500 μm.

The torque holding the plate at the prescribed angle is due to the field of the permanent magnet in the absence of current, while the actuation torque necessary to switch the plate angle is due to the field variation caused by a current pulse in the conductors. The field analysis problem consists of finding the magnetic field distribution for a given plate angle. In this respect, a typical finite-element mesh is composed of 2,300 triangles; second-order polynomial Lagrangian elements are considered, originating approximately 75,000 unknowns [21]. The corresponding torque-angle curve (Fig. 8) has been computed based on the virtual work principle.

In turn, the design problem reads: having prescribed lower thresholds for holding and actuation torque, given the plate angle $\phi = 10°$, *find the geometry of magnet and conductors, as well as the amplitude of the current pulse, such that the power loss in the conductors and the magnet volume are both minimized*. From the viewpoint of computational cost, it can be remarked that the evaluation of magnet volume wx_1x_2 and power loss $wx_7^2(\sigma x_4 x_5)^{-1}$ with $\sigma = 6\ 10^7$ Sm^{-1} is immediate, while the evaluation of both holding and actuation torque at $\phi = 10°$ is field dependent. In order to deal with feasible design configurations, suitable geometric constraints have been considered; moreover, the upper bound $x_7(x_4x_5)^{-1} < 5\ 10^9$ Am^{-2} have been fulfilled for the pulsed current density.

An approximation of the Pareto front in the power-loss *vs* magnet-volume space is shown in Fig. 9. The initial number of individuals processed was set to 20; the optimization procedure was stopped after 40 generations.

VI. CASE STUDY: INDUCTION HEATING OF A GRAPHITE DISK

Induction heating is used in various industrial processes, because it is able to localize the heat sources inside the workpiece with high efficiency and good temperature control. In Silicon wafer production - which is a preliminary step in MEMS fabrication - there is the need of achieving a prescribed temperature distribution in the graphite disk supporting the wafers. Specifically, an industrial equipment used for the epitaxial growth of Si wafers is considered; a typical chemical-vapour-deposition (CVD) reactor system is shown in Fig. 10.

Epitaxial growth of Silicon requires that the susceptor, *i.e.* the graphite disk that is heated by induction, reaches a

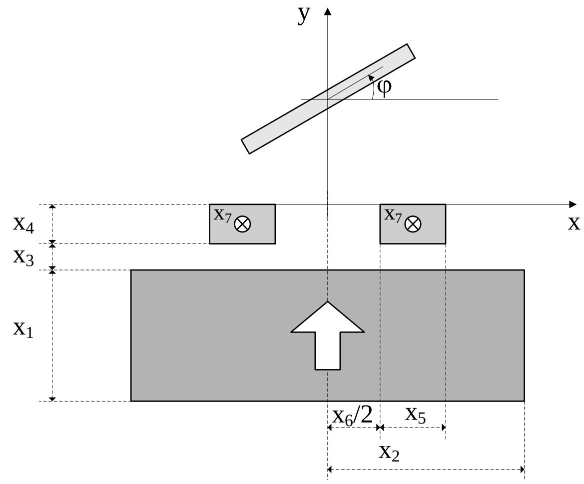

Fig. 7 Geometry of the magnetic MEMS and design variables: x_1 magnet height, x_2 magnet length, x_3 magnet air-gap, x_4 conductor height, x_5 conductor length, x_6 conductor air-gap, x_7 current pulse amplitude. The plate gravity-centre is located 500 μm above the x axis.

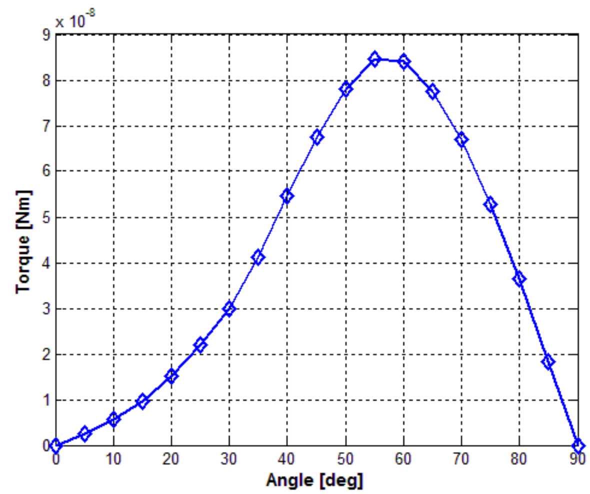

Fig. 8 Holding torque *vs* angular position ϕ for the device shown in Fig. 7, when x_7=0. Geometric data: x_1 = 100 [μm], x_2 = 1.2 [mm], x_3 = 50 [μm], x_4 = 50 [μm], x_5 = 200 [μm], x_6 = 600 [μm], x_7 =10 [A], plate length = 1 mm, plate height = 25 μm.

working temperature of 1050 - 1100 °C at steady state. Obtaining a good level of thermal uniformity is not easy; in fact, no power is induced in the disk region close to the axis, while the external edge of the disk has not enough power to compensate the losses due to convection and radiation.

The design of the inductor heating the disk implies the solution of coupled electromagnetic and thermal fields, along with the use of optimal design procedures to identify the best possible device or process. An approach in terms of multiobjective design is presented with reference to a particular induction heating system [12].

The inductor winding exhibits 3 groups of 4 circular and plane turns (so-called pancake inductor); all turns are series connected and carry a current of 1 kA$_{rms}$ at 1 kHz. Fig. 11 shows 1/12 of the three-dimensional model of the inductor with the graphite disk to heat; the design variables are also represented: they are the mean radius R_k of each group of

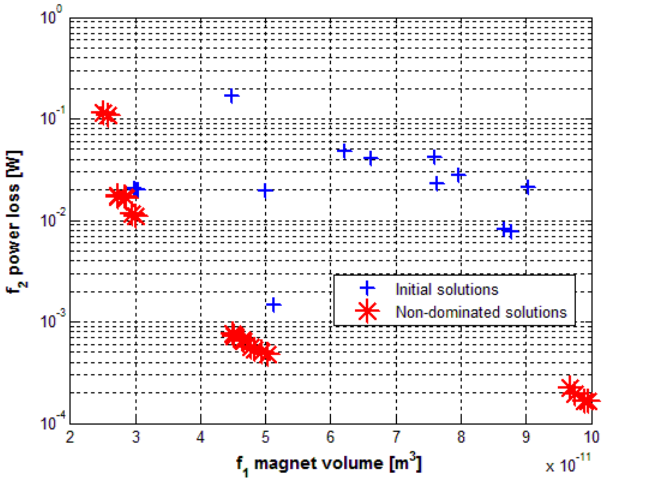

Fig. 9 Optimization results in the volume-loss space (20 individuals, 40 generations). Constraints: holding torque > 1 nNm, actuation torque > 0.25 nNm.

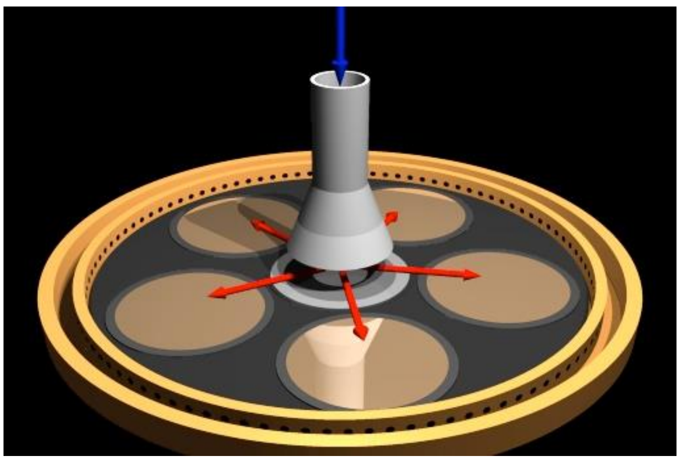

Fig. 10 A CVD reactor system driving the epitaxial growth of five Si wafers.

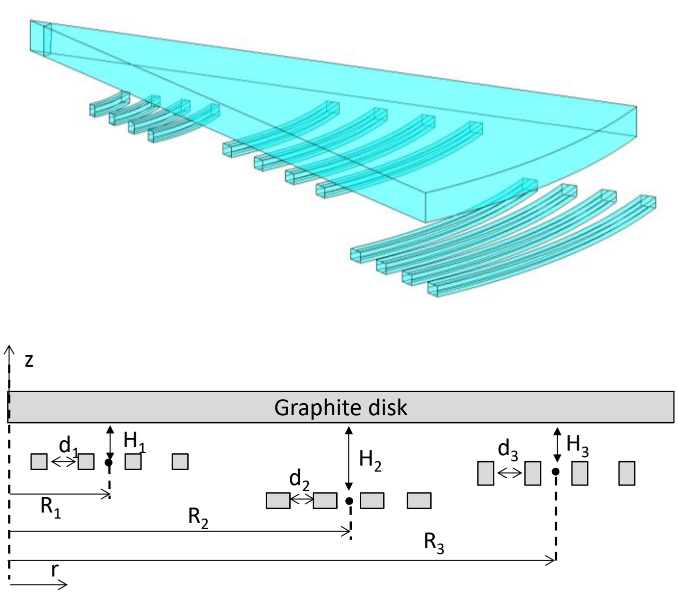

Fig. 11 Geometry of pancake inductor with design variables.

turns, the radial distance d_k between turns in each group, the axial distance H_k of each group from the disk ($k = 1,3$: in total, nine variables).

A. *Direct problem: multiphysics field analysis*

Even if the model is axial-symmetric, a 3D geometry is simulated for the sake of generality, eventually including a more complex model with non-symmetric effects. The electromagnetic (EM) problem is solved in time-harmonics conditions, in terms of $\overline{T} - \Omega$ formulation [4], in a domain including inductor winding, disk, and surrounding air. According to the latter, in the low frequency limit, magnetic field vector $\overline{H}$ and electric vector potential $\overline{T}$ differ by the gradient of a harmonic function Ω (magnetic scalar potential)

$$\overline{H} = \overline{T} - \overline{\nabla}\Omega \tag{8}$$

Since electric vector potential is used in conducting regions only, while magnetic scalar potential is used elsewhere, a save of computational cost is obtained. In time-harmonics conditions, the governing equations for complex vector $\dot{\overline{T}}$ and complex scalar $\dot{\Omega}$ in a domain D with boundary Γ follow:

$$\overline{\nabla}^2 \dot{\overline{T}} - j\omega\mu\sigma \dot{\overline{T}} = -\overline{\nabla} \times \dot{\overline{J}}_0 \tag{9}$$

with $\dot{\overline{J}}_0$ complex vector of impressed current density and σ electric conductivity, and

$$\nabla^2 \dot{\Omega} - j\omega\mu\sigma \dot{\Omega} = 0 \tag{10}$$

subject to appropriate boundary conditions.

The actual distribution of current in each turn, simulated as a solid conductor, is taken into account in order to evaluate the inductor efficiency in terms of the volume integral of the power density. Specifically, it is defined as the ratio of the active power transferred to the disk to the one supplied to both disk and winding:

$$\eta = \frac{\int_{\text{disk}} \sigma_d^{-1} \left\| \overline{\nabla} \times \dot{\overline{T}} \right\|^2 d\Omega}{\int_{\text{disk}} \sigma_d^{-1} \left\| \overline{\nabla} \times \dot{\overline{T}} \right\|^2 d\Omega + \int_{\text{winding}} \sigma_w^{-1} \left\| \overline{\nabla} \times \dot{\overline{T}} \right\|^2 d\Omega} \tag{11}$$

with σ_d and σ_w electrical conductivities of graphite and copper, respectively. In turn, the thermal problem is solved in steady state condition, assuming the power density in the disk, which is derived from the EM field analysis, as the source term. The thermal domain is the graphite disk, along the boundary of which a suitable condition of heat exchange holds. Values of both electrical and thermal conductivities are considered at the expected steady-state average temperature.

The governing equation for temperature T is the Fourier's equation at steady state:

$$-\overline{\nabla}\cdot\left(\lambda\overline{\nabla}\mathrm{T}\right)=\sigma^{-1}\left\|\overline{\nabla}\times\dot{\overline{\mathrm{T}}}\right\|^{2} \tag{12}$$

with λ thermal conductivity; along the disk boundary, the Fourier's equation is subject to the adiabatic condition at r = 0, and

$$-\lambda\frac{\partial \mathrm{T}}{\partial \mathrm{n}}=\mathrm{h}\left(\mathrm{T}-\mathrm{T}_0\right) \tag{13}$$

elsewhere; in (13) h is a thermal exchange coefficient incorporating the radiation loss effect, while T_0 is the environment temperature equal to 50 °C.

The numerical solution of the coupled electromagnetic and problem is based on a FEM tool [22] for three-dimensional field analysis; approximately, a typical solution mesh is composed of 130,000 linear tetrahedral elements.

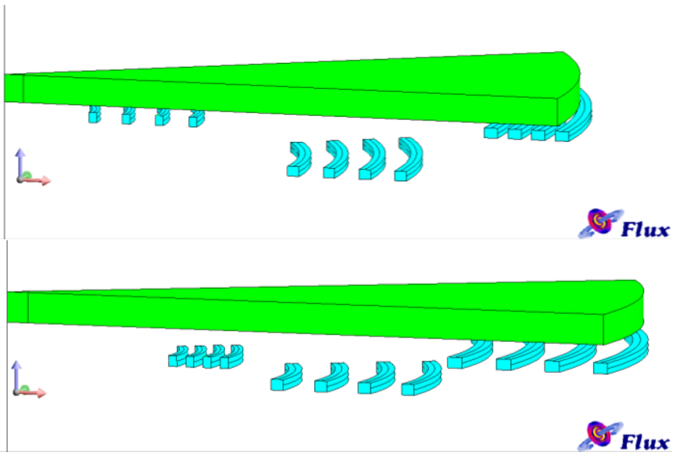

Fig. 13 Geometries of inductor corresponding to: (a) initial (start, f_1 = 0.139, f_2 = 155.79 °C), and (b) final temperature profile (stop_16, f_1 = 0.137, f_2 = 85.15 °C).

B. *Inverse problem: efficiency vs temperature optimization*

As far as the optimization problem is concerned, two design criteria have been defined. The complementary efficiency, 1-η, to be minimized, and the temperature discrepancy in the graphite disk at thermal steady state, to be minimized. Accordingly, the following objective functions have been implemented:

$$f_1(x)=1-\eta(x) \tag{14}$$

$$f_2(x)=T_{max}(x)-T_{min}(x) \tag{15}$$

where T_{max} and T_{min} are maximum and minimum temperature values along a radial line γ located 1 mm under the upper surface of the graphite disk, and x = (R_k,H_k,d_k) , k=1,3 is the design vector. In practice, both functions (14) and (15) have to be minimized with respect to design variables shown in Fig. 11.

Objective (14) refers to the magnetic domain, while objective (15) refers to the thermal one: a multiphysics and multiobjective optimization problem is so originated.

C. *Optimal design results*

Fig. 12 shows the approximated Pareto front of problem (15)-(16) after 10 (stop_10) and 16 (stop_16) iterations, respectively; an example of temperature profiles along the disk surface is also shown. The geometries of inductor winding, which correspond to initial and final temperature profiles, are shown in Fig. 13, while the relevant values are reported in Table II.

The initial solution (start) is a dominated one, while the final solution (stop_16) is located along the numerically-derived Pareto front. Apparently, there is an improvement of temperature uniformity on the disk surface without worsening

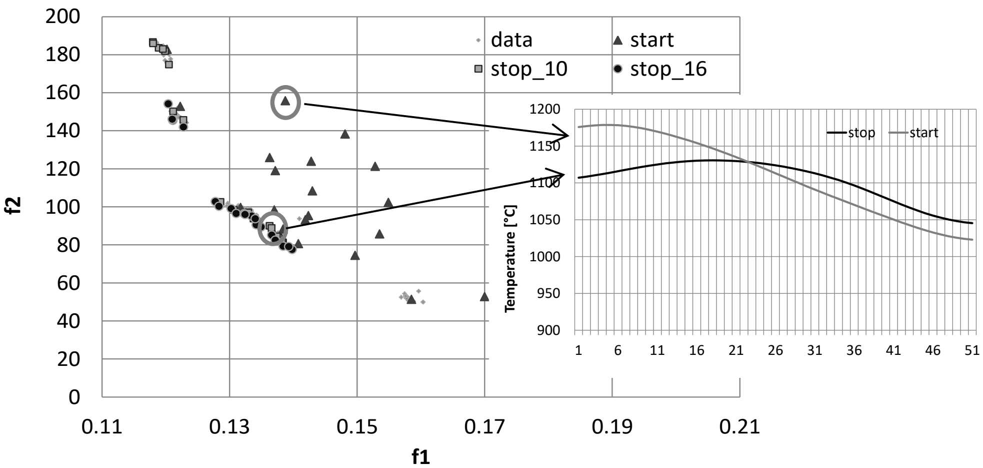

Fig. 12. Approximated Pareto front of problem (14)-(15) and example of initial (f_1=0.139, f_2=155.79 °C) and final temperature profile (f_1=0.137, f_2=85.15 °C).

TABLE II
DESIGN VARIABLES AND OBJECTIVE FUNCTION VALUES FOR THE GEOMETRIES IN FIG. 13.

	d_1 [mm]	d_2 [mm]	d_3 [mm]	H_1 [mm]	H_2 [mm]	H_3 [mm]	R_1 [mm]	R_2 [mm]	R_3 [mm]	f_1	f_2 [°C]
initial	13.47	12.73	5.43	25.89	3.00	26.88	72.57	179.54	273.70	0.139	155.79
final	4.35	15.14	16.58	17.02	7.96	21.03	92.94	162.98	253.05	0.137	85.15

the efficiency of the inductor-disk system. Indeed, the decision maker is free to select other Pareto-optimal solutions in Fig. 12 according to his or her preferences.

VII. Conclusion

While there have been significant improvements in the capabilities in the area of multiobjective optimal design, the uptake by industrial designers has been somewhat limited. There are, possibly, two reasons for this. The first is that the evidence, at the industrial level, that computer-based optimization processes can actually enhance a designer ability to create a better product has been lacking. The second relates to the fact that most optimization packages currently available only handle a single objective and a limited number of design variables. In fact, suitable optimization systems, with no restriction in the size of the design space to be explored, and with simple and flexible expressions of objectives and constraints, would help match the needs of the designer.

In the paper, three case studies were investigated, and the relevant field analysis problem was solved by means of FEM; standard resources in terms of personal computing were sufficient to make the Paretian optimal design work. The optimal design method proposed is valid in general; in fact, it works pretty well, independently of the direct-model equations considered: in principle, Maxwell-Fourier's equations or Maxwell-Fourier-Lamé's equations for MEMS, but also *e.g.* Schroedinger's equations of quantum electrodynamics, should a nanoscale physical domain be involved. Under this frame, the proposed approach puts the ground for a more general method devoted to the optimal shape design of any MEMS configuration; in fact, the application of multiobjective optimizations to this kind of devices is still at an early stage.

References

[1] Di Barba, P. (2010), Multiobjective Shape Design in Electricity and Magnetism, Springer.

[2] Bäck, Th. (1996), Evolutionary Algorithms in Theory and Practice, Oxford University Press.

[3] P. Neittaanmäki, M. Rudnicki, and A. Savini (1996), Inverse Problems and Optimal Design in Electricity and Magnetism, Oxford University Press.

[4] Di Barba, P., Savini, A., and Wiak, S. (2008), Field Models in Electricity and Magnetism, Springer.

[5] Di Barba, P. (2011), "Remarks on optimal design methods in electromagnetics", Intl Compumag Society Newletter, vol.18, no.2,.pp. 3-18.

[6] K. Deb (2001), Multi-Objective Optimization using Evolutionary Algorithms, Wiley.

[7] W.Tang, T. Nguyen and R. Howe, "Laterally driven polysilicon resonant microstructures", Sensors and actuators, vol. 20, 1989, pp.25-32.

[8] S. Wiak and K. Smółka, "Numerical modelling of 3-D comb drive electrostatic accelerometers structure (method of levitation force reduction)". COMPEL, vol.28, 2009, pp. 593-602.

[9] W.C. Tang, M.G. Lim and R.T. Howe, "Electrostatic Comb Drive Levitation and Control Method". J. Microelectromechanical Systems, vol. 1, 1992, pp.170-178.

[10] M. Boudaoud, Y. Haddab, and Y. Le Gorrec, "Modeling and Optimal Force Control of a Nonlinear Electrostatic Microgripper", IEEE/ASME Trans. Mechatronics, vol. 18, no. 3, pp. 1130–1139, 2013.

[11] R. Legtenberg, A.W. Groeneveld and M. Elwenspoek, "Comb-drive actuators for large displacements". J. Micromechanics and Microengineering, vol. 6, 1996, pp. 320.

[12] Di Barba, P., Dughiero, F., Lupi, S., and Savini, A. (2003), "Optimal Shape Design of Devices and Systems for Induction Heating: Methodologies and Applications", COMPEL, vol. 22, no. 1, 2003, pp. 111-122.

[13] Di Barba, P., and Lorenzi, A. (2013), "A magneto-thermo-elastic identification problem with a moving boundary in a micro-device", accepted for publication in *Milan J. of Mathematics*.

[14] M. Grossard, M. C. Rotinat-Libersa, N. Chaillet, and M. Boukallel, "Mechanical and control-oriented design of a monolithic piezoelectric microgripper using a new topological optimization method," IEEE/ASME Trans. Mechatronics, vol. 14, no. 1, pp. 32–45, 2009.

[15] L. Hu, K.-M. Lee, and X. Fu, "A method based on measured boundary conditions for reconstructing the magnetic field distribution of an electromagnetic mechatronic system", IEEE/ASME Trans.Mechatronics, vol. 15, no. 4, pp. 595–602, 2010.

[16] P. Favrat, L. Paratte, H. Ballan, M. J. Declercq, and N. F. de Rooij, "A 1.5-V-supplied CMOS ASIC for the actuation of an electrostatic micro-motor", IEEE/ASME Trans. Mechatronics, vol. 2, no. 3, pp. 153–160, 1997.

[17] M. Komori and T. Hirakawa, "A magnetically driven linear microactuator with new driving method", IEEE/ASME Trans. Mechatronics, vol. 10, no. 3, pp. 335–338, 2005.

[18] B. Delinchant, H.L. Rakotoarison, V. Ardon, O. Chabedec and O. Cugat, "Gradient based optimization of semi-numerical models with symbolic sensitivity: Application to simple ferromagnetic MEMS switch device", *IJAEM*, 30 (2009), 189-200.

[19] Yee-Pien Yang, Jieng-Jang Liu, Da-Hau Ye, Yi-Ruei Chen, and Pai-Hsiu Lu, "Multiobjective Optimal Design and Soft Landing Control of an Electromagnetic Valve Actuator for a Camless Engine", IEEE/ASME Trans. Mechatronics, vol. 18, no. 3, pp. 963–972, 2013.

[20] S. Kota, "Tailoring unconventional actuators using Compliant Transmisisons: Design Methods and applications", IEEE/ASME Trans. Mechatronics, vol. 4, no. 4, pp. 396–408, 1999.

[21] Comsol Multiphysics: www.comsol.com [last visited July 2013].

[22] Flux3D: www.cedrat.com [last visited July 2013].

[23] NSGA-II: www.iitk.ac.in/kangal/codes [last visited July 2013].

Paolo Di Barba, (M'95) DSc PhD MEng, is a full professor of electrical engineering at the University of Pavia (Italy), Department of Industrial and Information Engineering. His scientific interests include the computer-aided design of electric and magnetic devices, with special emphasis on the methods for field synthesis and automated optimal design. He has authored or co-authored more than 100 papers, either presented to international conferences or published in international journals, a book Field Models in Electricity and Magnetism (Springer, 2008) and a monograph Multiobjective Shape Design in Electricity and Magnetism (Springer, 2010).

Sławomir Wiak, DSc PhD MEng, is deputy Rector of the Łódź University of Technology (Poland). He is specialized in electrical and computer engineering, covering computer-aided design, modelling and simulation, data base and expert systems, mechatronics. He was an invited professor at the Université d'Artois (France) and University of Pavia (Italy). He is a member of scientific societies: IEEE, International Compumag Society, Polish Society of Applied Electromagnetics. He has authored or co-authored more than 350 papers and 18 monographs and text books. He cooperates with the University of Southampton (UK), National Technical university of Athens, University of West Bohemia in Plzen, University of Prague, Czech Academy of Sciences, University of Maribor (Slovenia), University of Vigo (Spain). He is the general chairman of the International Conference on Electromagnetic Fields in Mechatronics, Electrical and Electronic Engineering (ISEF).